# Nanomaterial identification of powders: comparing volume specific surface area, X-ray diffraction and scanning electron microscopy methods

Claire Dazon, Olivier Witschger, Sébastien Bau, Vanessa Fierro, Philip Llewellyn

# Nanomaterial identification of powders: comparing Volume Specific Surface Area, X-Ray Diffraction and Scanning Electron Microscopy methods

Claire Dazon,*[a], Olivier Witschger, [a] Sébastien.Bau, [a] Vanessa.Fierro, [b] and Philip.L. Llewellyn [c]

[a] Laboratoire de Métrologie des Aérosols, Institut National de Recherche et de Sécurité (INRS), Vandœuvre, France (*Email: claire.dazon@inrs.fr; Tel : +33 83 50 20)

[b] Institut Jean Lamour - UMR CNRS 7198, Epinal, France

[c] Aix Marseille University, CNRS, Laboratoire MADIREL, Marseille, France

Nanomaterials in powder form are widely produced and used in numerous applications. Nanomaterial identification is a growing concern for several areas encountering these substances. The current reference criterion of the European Commission (EC) for nanoparticle identification is the number size distribution of the constituent particles. One example of how the latter can be obtained is by Electron Microscopy (EM) method. However, this method is not widely available and is time-consuming to perform and analyse. Alternative methods, such as Volume Specific Surface Area (VSSA), allows also a nanomaterial identification. VSSA is the product of the external specific surface area of the powder by its skeletal density and appears to be adapted more specifically for powders. The techniques required to measure the two parameters used to calculate VSSA are more widely available than EM, but sample preparation can be delicate. Futhermore, deeper evaluation of the reliability of VSSA for nanomaterial classification as well as a more detailed characterization methodology for its implementation and discussion about the relative merits of this method versus EM are still necessary. Here, we determined, through a detailed and operational characterization strategy, the VSSA for seven metal oxides powders (4 $TiO_2$, 1 $SiO_2$, 2 $CaCO_3$) and an activated carbon, all of them being produced at industrial scale. These eight samples covered a range of constituent particle sizes between 10 nm and 18 µm. Equivalent particle sizes determined by VSSA, X-Ray Diffraction (XRD) (another method giving access to an equivalent particle size and integrated in our characterization methodology) and Scanning Electron Microscopy (SEM) (reference method) were compared. The results showed that VSSA can robustly identify nanomaterials in the form of powders (-12% mean bias on equivalent particle sizes relative to SEM).

## 1. Introduction

Nanomaterials are now a large industry [1-3]. The improvement and increasing control of synthesis processes as well as the new properties of materials developed at the nanoscale suggest that this area is expected to continue to grow.

Whatever the application and the context, the identification of the "nano" nature of substances is an essential step. For example, when implementing the chemical registration dossiers in Europe (REACH regulation) [4], nanomaterials match the definition of "substances" and therefore, identification and information provisions for them are applicable. Similarly, the responsible management of risks associated to nanomaterials in the workplace requires their identification to propose preventative measures [5, 6].

Boverhof *et al* [7] focused on available nanomaterial definitions in the regulatory context worldwide and pointed out a lack of harmonization. By consequence, it is important to indicate the nanomaterial definition used when characterizing any substance. In 2011, the European Commission (EC) issued a recommendation on the definition of nanomaterials related to legal classification [8]. As explained by Gao and Lowry [9], this recommended EC definition, "provides the most specific measurable parameters of nanomaterials compared to other definitions", that is why it appears that several areas rely on this recommendation for the solely nanomaterial identification. A substance is considered as a nanomaterial since at least 50% of the constituent particles in the number size distribution have one or more external dimensions between 1 nm and 100 nm. To determine this distribution, the EC recommends implementing the best available methods and the most appropriate and harmonized protocols as possible. Electron Microscopy (EM) methods are widely harnessed in this view since they let have a direct characterization of particle size and shape [10, 11]. However, these methods are time consuming and require significant human and material resources for both imaging and post-hoc analysis.

Another possibility proposed by EC to identify nanomaterials relies on the determination of the Volume Specific Surface Area (VSSA) when possible. This parameter was suggested as an alternative when defining nanomaterials to overcome disadvantages related to size measurements. The VSSA (equation 1) of a material is calculated from the external specific surface area ($A_{Ex}$) and the material's skeletal density ρ:

$$VSSA\ (m^2/cm^3) = A_{Ex}\ (m^2/g) \times \rho\ (g/cm^3) \quad (1)$$

Based on its VSSA, a substance is considered as a nanomaterial: "when it presents a volume specific surface area greater than 60 $m^2/cm^3$" [8]. This limit of 60 $m^2/cm^3$, also named $VSSA_{Cutoff}$, corresponds to the VSSA of monodisperse spherical non-porous particles with a density of 1 $g/cm^3$ and a diameter of 100 nm. The $VSSA_{Cutoff}$ has been recently discussed for adapting the threshold value according to the particle shape (40 $m^2/cm^3$ for fiber-like particles or 20 $m^2/cm^3$ for platelets [12]). However, in the absence of consensus, the threshold of 60 $m^2/cm^3$ remains the $VSSA_{Cutoff}$ to consider when applying EC recommendation for nanomaterial identification. Moreover, if a material is identified as non-nanomaterial with its VSSA, particle sizing remains mandatory to confirm the previous statement.

The VSSA method is a particularly attractive approach since it is relatively well adapted for powders. Indeed, for a powder, the $A_{Ex}$ can be determined by the relevant gas adsorption method [13-15]; and the skeletal density of the material can be obtained by Helium pycnometry [16]. These two methods are less expensive overall and more readily available than EM. Above all, powders are increasingly encountered in industry and laboratories (synthesis and/or use) as they are included in the composition of products across a very wide range of activity sectors: building, food and agriculture, cosmetics, energy, and so forth. The 2016 public R-Nano report indicates that almost 475,000 tons of nanomaterials were manufactured, distributed or imported in France [17]. Thus, there is an increasing need for nanomaterial identification for regulation purpose, process control, as well as risk assessment. Therefore, the relative easier accessibility of VSSA could be an interesting solution to identify nanomaterials.

Although gas adsorption and Helium pycnometry are relatively widely available, precise sample preparation and rigorous data analysis are necessary. Both techniques need a sample outgassing to limit underestimation of measured values [18-22, 34]. The $A_{Ex}$ determination requires an accurate selection of the models (BET for non porous, macroporous or mesoporous powders, t-plot model for microporous powders) as explained by Lecloux [23] and Wohlleben *et al* [24] in their works about the use of VSSA for nanomaterial classification. Besides, skeletal density measured by Helium pycnometry can be validated by comparison with the material's theoretical density, based on its theoretical chemical and crystallographic composition.

To date, the Nanodefine European project [25] allowed advances in the assessment of the relevance of VSSA for the classification of powders as nanomaterials. This project particularly focused on industrial powders representative of the most frequently encountered materials. However, it is still necessary to evaluate the reliability of VSSA for nanomaterial powder identification for promoting this parameter as an alternative approach when EM methods are not available. Besides, in spite of SOPs and guides availability, an operational strategy for VSSA

implementation, notably accessible for non-specialists of material characterization, is manifest. Furthermore, it would be interesting to discuss the relative merits of VSSA versus EM methods.
In this context, our study aimed to bring new results supplementing those of the Nanodefine European project for nanomaterial identification. In particular, a detailed operational approach was applied to a series of representative industrial powders to determine their VSSA and state whether they have to be considered as nanomaterials. The relevancy of the classification of powders by VSSA is evaluated by comparing the corresponding equivalent particle size with the Scanning Electron Microscopy (SEM) reference method and with the equivalent particle size derived from X-Ray Diffraction (XRD).

## 2. Materials and Methods

### 2.1. Materials

The eight powders used in this study are presented in Table 1. The metal oxides $TiO_2$, $SiO_2$ and $CaCO_3$, seven in total, represent the most frequently encountered materials in France according to the latest R-Nano report (2016), with recorded quantities exceeding 1000 tons. That is why we selected them as we considered these materials are representative of powders potentially found in workplaces. These metal oxides are produced at industrial scale and are used in products with applications in engineering, food and agriculture, cosmetics, paints and varnishes, energy and even textiles. In addition of the metal oxides, a powdered activated carbon Maxsorb® which is used for its high specific surface area (> 3000 m²/g) mainly for gas storage by adsorption [26] was chosen. These powders were selected based on the $A_t$ indicated by their de-identified suppliers, which covered a broad range from a few tens of m²/g to more than 3000 m²/g.

**Table 1** Physico-chemical characteristics of the industrial powders studied, as indicated by suppliers.

| Powder | Code | Supplier | $A_t$ Supplier (m²/g) | Purity (Wt %) |
|---|---|---|---|---|
| $TiO_2$ | LSSA | A | 10 | 99 |
| | MSSA | | 90 | 99 |
| | HSSA | | 350 | 99.5 |
| | P25 | B | 50 | 99 |
| $SiO_2$ | $SiO_2$ | C | >600 | 99.5 |
| $CaCO_3$ | $CaCO_3$ A | D | n.a | 97.5 |
| | $CaCO_3$ B | | | 94.5 |
| Activated Carbon Maxsorb® | MSC-30 | E | >3000 | 99 |

### 2.2. Characterization approach

The industrial powders were characterised by the approach schematized in figure 1.
This strategy can be broken down into three phases.

#### 2.2.1. Phase 1 (P1)

The first phase consists in implementing the following four characterisation methods in parallel: thermogravimetric analysis (TGA), chemical analysis, XRD and SEM.

- TGA allows an optimised outgassing protocol to be selected for sample preparation before the gas adsorption and Helium pycnometry measurements when seeking to calculate the powders' VSSAs.
- Chemical analysis by X-ray fluorescence, ICP-MS or ICP-OES, or alternatively the supplier's data allow the material's composition to be included when selecting the theoretical density $\rho_{th}$ to be compared to the $\rho$ measured by Helium pycnometry, for validation of the experimental results.
- XRD allows determining the crystal structure of the particles making up the powder as well as their proportions. Moreover, it is possible to calculate a mean particle size $d_{XRD}$ by applying the Scherrer formula (equation 2):

$$d_{XRD} = \frac{0{,}9\lambda}{\theta cos\beta} \quad (2)$$

Where λ is the wavelength of the X-ray in nm, θ is the Bragg angle for the diffraction peak used for the calculation. The angle with the greatest radian intensity is generally selected. β is the full-width at half-maximum of the selected diffraction peak, in radians.
This formula is based on the hypothesis that the particles are spherical or cubic and monocrystalline and appears to be appropriate for crystal sizes greater than 10 nm [27].
The crystal structure is also considered when selecting the theoretical density of the material to be compared to the density measured by Helium pycnometry for validation of the experimental results.

- SEM can be used to determine the main shape of the constituent particles in the powder, making it possible to choose a D factor from which a cutoff VSSA value can be defined ($VSSA_{Cutoff}$) as proposed by Wohlleben *et al* [24]. In addition, SEM can be used to establish the size distribution of the constituent particles in the powder when the number of identifiable and isolated particles on the acquired images is sufficient, i.e., at least 100 to 200 particles [28, 29]. The size of the measured particles corresponds, most of the time, to the mean Feret diameter [29, 30] or to the projected equivalent surface diameter $d_S$ of a disc of area S according equation 3 for spherical particles:

$$d_S(nm) = 2\sqrt{\frac{S}{\pi}}\ (nm^2)\ (3)$$

For particles in the form of fibres (D = 2), the diameter, rather than the length of the fibre, is measured. For particles in the form of platelets (D = 1), the thickness is measured. In this work, $d_{SEM}$ corresponds to $d_S$ for spherical particles, the diameter of a fibre for fibre-like particles or the thickness of platelets.

#### 2.2.2. Phase 2 (P2)

The second step is to determine the VSSA by performing gas adsorption and Helium pycnometry measurements on outgassed samples, prepared by the optimised protocol selected following the thermogravimetric measurements.

#### 2.2.3. Phase 3 (P3)

The third step is data analysis.

##### 2.2.3.1. Gas adsorption

The gas adsorption isotherms are compared to the typical isotherms proposed by IUPAC [14] so as to apply:

- The BET model when a type II (non-porous or macroporous material) or type IV (mesoporous material) isotherm is obtained, for which $A_{Ex} = A_t$. This model is the easiest to apply and the most relevant for these types of isotherm [31].
- The t-plot model is applied when a type I (microporous model) isotherm is obtained, it extracts the $A_{Ex}$ from the $A_t$ for microporous materials. Rouquerol *et al.* [32, 33] described how the calculation for the t-plot method should be applied from the values for the Boer "universal t curve" obtained for a non-porous alumina. This reference is the most frequently used to determine the $A_{Ex}$ for microporous materials using the t-plot model and is the one used in this work.

##### 2.2.3.2. Helium pycnometry

Measurements of the skeletal density ρ by Helium pycnometry were compared to the theoretical values $\rho_{th}$ selected based on the chemical and crystallographic data available for the powders. The measurements were validated by verifying that the relative difference between ρ and $\rho_{th}$ was less than 10%, which corresponds to the uncertainty of the pycnometry measurement.

##### 2.2.3.3. Determining the VSSA and comparing equivalent particle diameters

The VSSA was calculated (equation 1) from validated $A_{Ex}$ and skeletal density data and compared to the $VSSA_{Cutoff}$, which was selected on the basis of the particle shapes observed in SEM images (D factor).

The equivalent mean diameter $d_{VSSA}$ of the particles making up the powder was calculated from the value of the VSSA and the D factor (equation 4):

$$d_{VSSA}(\mu m) = \frac{2D}{VSSA(m^2/cm^3)} \quad (4)$$

The mean diameters obtained by the three characterisation methods for size measurement: VSSA ($d_{VSSA}$), XRD ($d_{XRD}$), SEM ($d_{SEM}$) were then compared to the size determined by SEM, with an arbitrarily determined relative bias tolerance of ± 15% corresponding to the maximum rounded absolute average bias we obtained in the comparison of VSSA and SEM. As the $d_{SEM}$ is the reference diameter, the ultimate classification of the powder as a nanomaterial or not was based on that value. The comparison of equivalent particle size lets validate the nanomaterial classification based on the solely VSSA value.

### 2.3. Experimental

For each characterisation method in the approach, the experimental details and additional explanations are provided hereafter.

#### 2.3.1. TGA

In this work, thermogravimetric analyses were performed with a thermobalance (Q500, TA Instruments). Samples were heated from room temperature (RT) up to 600 °C with a 10 C/min slope under argon at 100 mL/min. The TGA results directly affected how gas adsorption and Helium pycnometry were implemented during the characterisation approach. As a result, details of the TGA results are presented in the gas adsorption and Helium pycnometry paragraphs.

Before performing gas adsorption measurements, it is important to outgas the samples so as to eliminate the chemical species that may be adsorbed on the (external and internal) surfaces of the particles as water or atmospheric pollutants. Otherwise, $A_t$ measurements might be underestimated due to the presence of previously adsorbed molecules [13]. Outgassing is also required prior to measurement of the skeletal density by Helium pycnometry. The appropriate outgassing protocol can be selected by thermogravimetric analysis of the powder, whereby the powder sample is submitted to a temperature range, with addition of a neutral sweeping gas such as nitrogen or argon (to avoid chemical reactions between molecules and the powder). The sample's mass is monitored during the heating programme. The sample is considered "cleaned" when the mass variation as a function of time reaches a plateau that is maintained for at least 30 minutes. Before gas adsorption, powders are generally outgassed for at least 1 hour under a given vacuum, at the temperature corresponding to the one at which the mass variation plateau was attained in thermogravimetry. When elaborating the outgassing protocol before gas adsorption, one can chose for instance, the outgassing temperature corresponding to the beginning of plateau observation obtained with TGA.

However, thermogravimetry does not exactly reproduce the vacuum conditions implemented when outgassing powders before gas adsorption. In addition, although recommended, it is important to ensure that the samples are not degraded by the vacuum and the temperature applied during outgassing. A visual inspection is generally sufficient. A change in colour or appearance of the powder indicates that the sample has become degraded and that the outgassing procedure must be reviewed, such as by reducing the degassing temperature or extending its duration.

#### 2.3.2. XRD

XRD measurements were performed with a Siemens-Bruker AXS D5000 diffractometer in Bragg-Brentano configuration (coupled mode θ-2θ) with Cu- Kα radiation (wavelengths $K_\alpha 1$ = 0.15444 nm and $K_\alpha 2$ = 0.15406 nm with a $K_\alpha 1/K_\alpha 2$ wavelength ratio = 0.5). The proportions of the phases and the size of the crystalline domains were assessed using FullProf software (version 2015 for Windows, available at https://www.ill.eu/sites/fullprof/) based on the Rietveld method and by applying the Scherrer formula (equation 2).

#### 2.3.3. Chemical analysis

In this work, it was not possible to perform chemical analysis to determine chemical powder compositions. So, we used the chemical compositions in major elements (% weight) given by the various suppliers (see Table 1) were used when selecting the theoretical densities.

#### 2.3.4. SEM

EM images were acquired with a Zeiss Ultra-Plus Scanning Electron Microscope linked to a Bruker Quantacs 400 Energy Dispersive Spectrometer (EDS). Powder samples were deposited on aluminium pins covered with carbon tape (G3347N, Agar Instruments). The pins were then exposed to a metallizer (Denton Desk V) for 45 minutes to deposit carbon in order to make the samples conductive. Between 15 and 20 images were collected at 2 kV with magnifications between x 10,000 and x 500,000. A mean particle size $d_{SEM}$ was calculated as fewer than 50 particles could be counted on all the images obtained for each powder. Images were treated using Image J software (Java version 1.8.0).

#### 2.3.5. Gas adsorption

Gas adsorption measurements were performed with an automatic adsorption equipment (TRIFLEX, Micromeritics) with nitrogen as probe gas, at 77 K. As TGA analyses showed that all the samples were heat-stable over the RT–300 °C interval at atmospheric pressure, and this range is compatible with water and surface pollutants desorption, previously adsorbed onto the received powder materials. The selected outgassing temperature was 150 °C (mean temperature at which the mass variation plateau was measured) under vacuum ($10^{-2}$ mmHg) for a minimum of 24 hours. Only activated carbon was heated to 250 °C due to the known (but unquantified) microporosity of carbon. Indeed, microporous powders must be outgassed for longer time and/or at higher temperature to eliminate the species adsorbed in the narrow micropores [13]. All measurements were performed in triplicate on new samples. The $A_{Ex}$ for powders were then calculated by applying the analytical procedure explained in phase 3 of the characterisation approach.

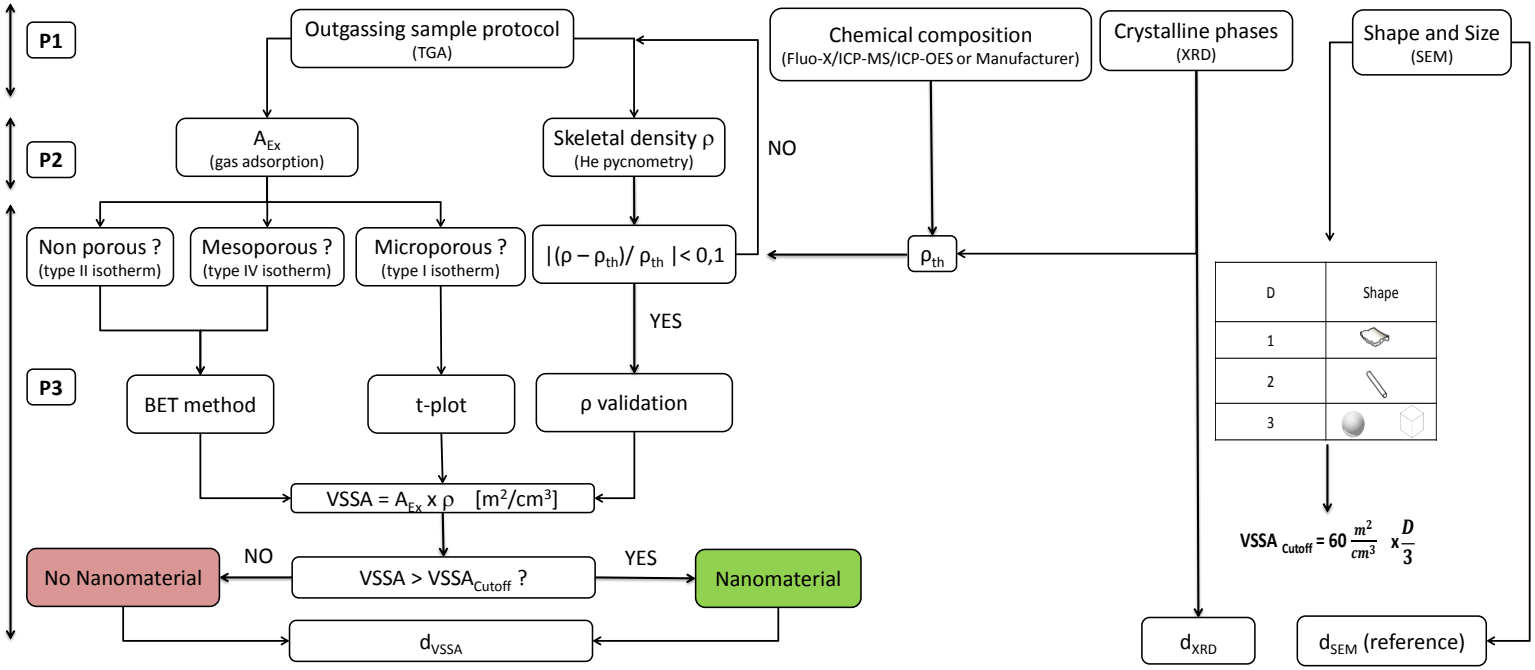


Comparison of $d_{VSSA}$ vs $d_{SEM}$ and $d_{XRD}$ vs $d_{SEM}$ to evaluate relevancy of VSSA and XRD for nanomaterial identification

**Fig. 1** Diagramme schematizing the general approach used in this work to determine the VSSA of powders and comparison with the XRD and SEM (reference) methods for nanomaterials identification.

#### 2.3.6. Helium pycnometry

The skeletal densities of the powders were determined by Helium pycnometry (Accupyc 1340, Micromeritics) in triplicate, with prior calibration of the measurement cell, as recommended by the manufacturer. Samples were dried in an oven at 105 °C overnight before performing measurements. The system used was incompatible with drying under vacuum, therefore samples were cooled in a desiccator and Helium pycnometry experiments were performed immediately after cooling to limit adsorption of water and other atmospheric gases. Experimental density measurements were validated by comparing the results obtained to the theoretical densities, taking the theoretical chemical compositions of the powders and their crystal structures (and proportions), as determined by XRD, into account.

## 3. Results and discussion

The results of this work are presented in the order of the characterisation approach used (see figure 1).

### 3.1. XRD, chemical composition and densities

The XRD and Helium pycnometry results are presented together in Table 2.

The crystal phases of powders are indicated along with their mass proportions. $TiO_2$ powders LSSA, MSSA and HSSA have a 100% anatase structure, $TiO_2$ P25 is an anatase/ rutile mixture with mass proportions 87/13. The two $CaCO_3$ have a 100% calcite structure. The crystal phases detected were those expected for these materials. $SiO_2$ and activated carbons, as MSC-30, powders are amorphous materials. By combining the crystallographic results with the chemical composition of the powders indicated by the suppliers, the theoretical densities can be selected for comparison with the skeletal densities measured by Helium pycnometry for validation. The powders studied here were considered pure to between 94.5 and 100% (Table 1). The theoretical densities for each powder therefore corresponded to the density of the corresponding raw materials. In the case of $TiO_2$ P25, the theoretical density combines that of anatase and rutile taking the mass ratio of each crystal phase into consideration. The theoretical densities used for the comparison were taken from the Handbook of Chemistry and Physics (96th edition).

Compared to the theoretical densities, most of the skeletal densities measured by Helium pycnometry displayed biases of less than 10%. These skeletal densities were therefore validated and used to calculate the VSSA. The bias in the skeletal densities measured was greater for two powders - $TiO_2$ HSSA (- 13.5%) and MSC-30 (+ 17.3%) - these bias values were attributed to insufficient degassing prior to analysis, perhaps due to the fact that the powder samples were not placed under vacuum before the Helium pycnometry measurements with the Accupyc 1340 device. Thus, for these two powders, the theoretical density was used to calculate the VSSA.

### 3.2. SEM

Figure 2 shows representative SEM images for each of the powders at different magnifications for comparison at the 100 nm scale except for the activated carbon and $CaCO_3$ A. For all the powders we observed that the constituent particles were extensively agglomerated, but individual particles remained sufficiently distinguishable to allow at least 50 particles to be measured, although in many cases measurements may have been imprecise. $TiO_2$ P25 was made up of spherical particles corresponding to the anatase phase. The rutile particles would have been characterised by a rod-like shape on the SEM images, but they were impossible to identify. Given the mass proportions of the crystal phases of anatase (87%) and rutile (13%) for $TiO_2$ P25, it was assumed that only the anatase particles were counted. The $CaCO_3$ A and MSC-30 powders have particles in the form of platelets, the other powders are composed of spherical particles. Consequently, the value D = 1 gives a $VSSA_{Cutoff}$ of 20 $m^2/cm^3$ for $CaCO_3$ A and MSC-30 whereas D = 3 gives a $VSSA_{Cutoff}$ of 60 $m^2/cm^3$ for the other powders.

**Table 2** Crystal phases of the powders, their mass proportions as measured by XRD, and skeletal densities measured by Helium pycnometry. Values are indicated with one standard deviation.

| Powder | Code | Crystal Structure | Proportions (% weight) | ρ g/cm$^3$ | $\rho_{th}$ g/cm$^3$ | Bias ρ % |
|---|---|---|---|---|---|---|
| $TiO_2$ | LSSA | Anatase | 100% | 3.87 ± 0.01 | 3.92 | -0.7 |
| | MSSA | | | 3.71 ± 0.01 | | -4.8 |
| | HSSA | | | 3.37 ± 0.01 | | -13.5 |
| | P25 | Anatase | 87% | 3.83 ± 0.01 | 3.94 | -2.7 |
| | | Rutile | 13% | | | |
| $SiO_2$ | $SiO_2$ | Amorphous | 100% | 2.07 ± 0.02 | 2.2 | -5.7 |
| $CaCO_3$ | $CaCO_3$ A | Calcite | | 2.71 ± 0.01 | 2.71 | 0 |
| | $CaCO_3$ B | | | 2.57 ± 0.01 | | -0.7 |
| Activated Carbon Maxsorb® | MSC-30 | Amorphous | | 2.58 ± 0.01 | 2.2 | 17.3 |

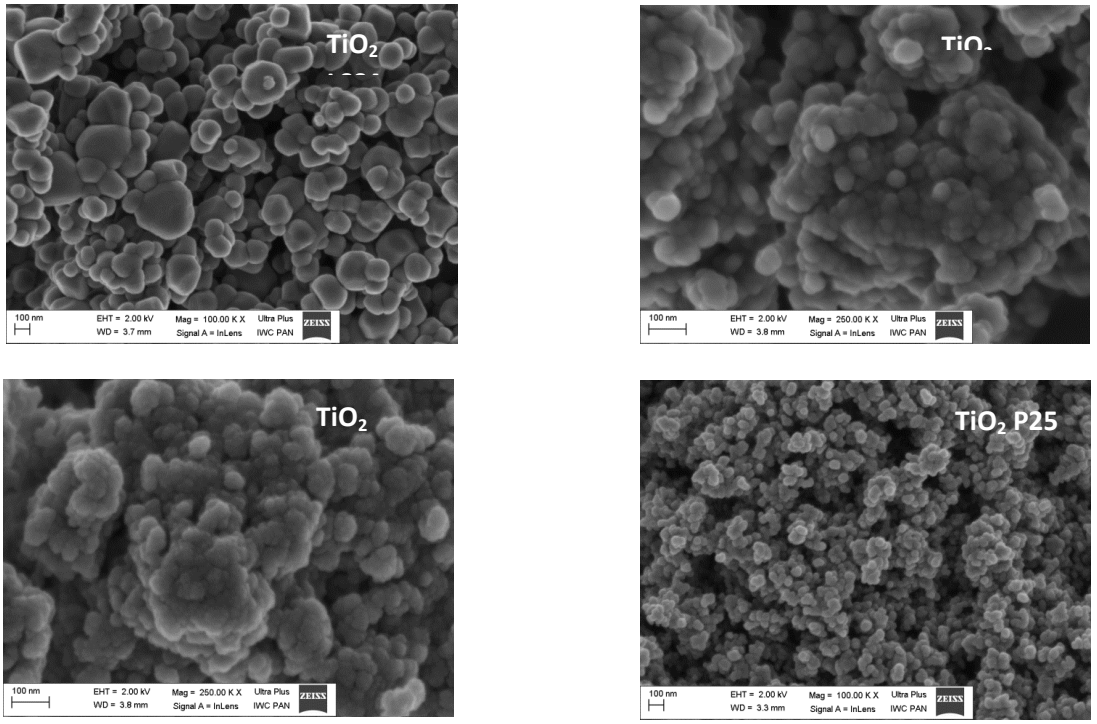


**Fig. 2** SEM images of the powders studied in this work.

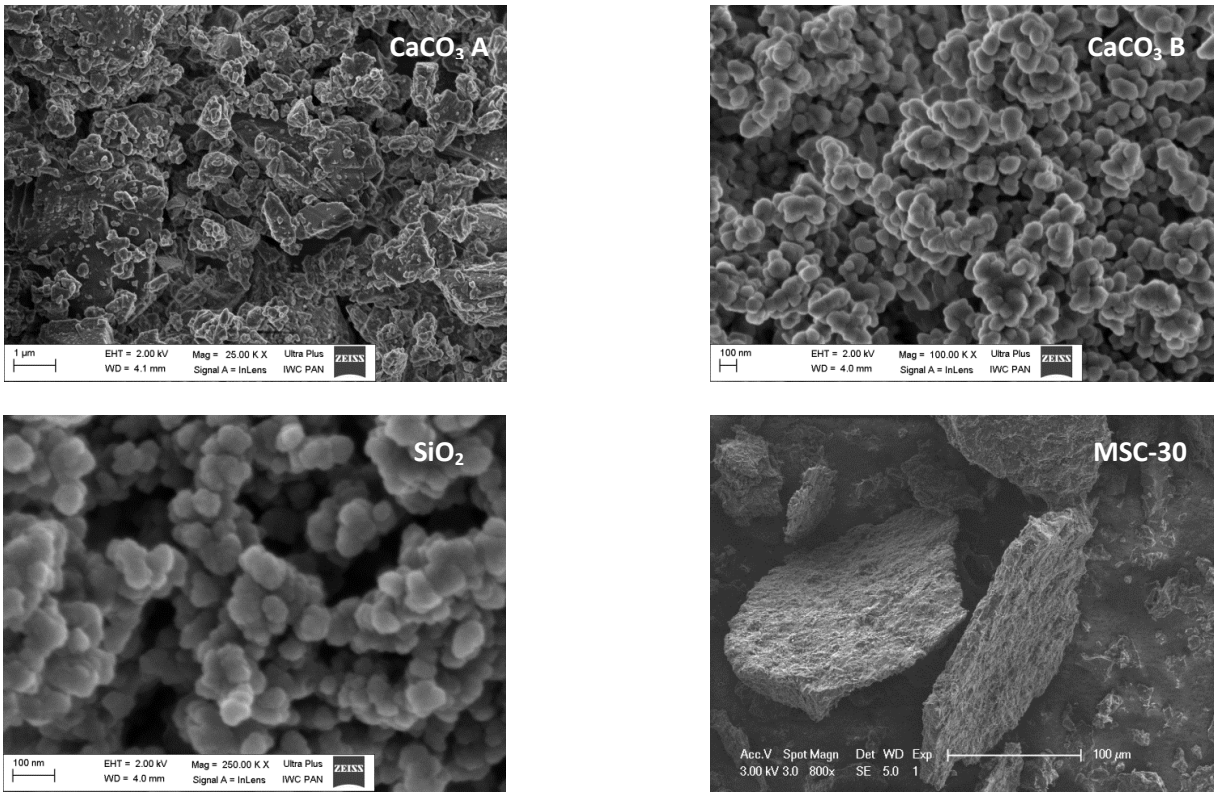


**Fig.2** *(continued)*

### 3.3. Specific surface area and VSSA

Figure 3 shows the nitrogen adsorption isotherms for $TiO_2$ MSSA and $SiO_2$. These adsorption isotherms were selected to demonstrate the most operational approach for analysis of the nitrogen adsorption isotherms for industrial powders. These adsorption isotherms were determined to be of type II for $TiSO_2$ MSSA and composite type I (b) +II for $SiO_2$, based on the reference isotherms proposed by IUPAC [14].

The BET model was used to calculate $A_{Ex}$ for the $TiO_2$ MSSA sample. This choice is obvious as the $TiO_2$ MSSA isotherm is equivalent to that of the IUPAC type II isotherm. In contrast, the calculation is more difficult for $SiO_2$ as its isotherm combines a type I (b) and a type II form. Figure 4 shows for relative pressures P/P° between $10^{-6}$ and $10^{-3}$, nitrogen adsorption for silica varies between 0 and 6 mmol/g. This represents a significant gas adsorption (almost 30% of the total) covering three orders of magnitude, as a result, we applied the t-plot model to calculate the $A_{Ex}$ [33, 34]. From these observations, we can conclude that the microporous surface of this silica represents 85% of the total surface area.

The other nitrogen adsorption isotherms can be found in the Supplementary Information. The isotherms obtained for $TiO_2$ LSSA and P25, and those for $CaCO_3$ A and B were type II (non-porous or macroporous) whereas that for $TiO_2$ HSSA corresponded to a composite I (b) and II isotherm. MSC-30 presented a type I (b) adsorption isotherm. The BET model was therefore applied for $TiO_2$ LSSA and P25, $CaCO_3$ A and B powders, whereas the t-plot model was selected for $TiO_2$ HSSA and MSC-30.

Table 3 lists the $A_{Ex}$, the D factor determined by SEM, the $VSSA_{Cutoff}$ and the VSSA for the powders studied. Values are indicated ± 1 standard deviation. Powders for which the VSSA is greater than the $VSSA_{Cutoff}$ are considered nanomaterials according to this method, they are indicated by a green background. The powders not identified as nanomaterials are indicated by a red background.

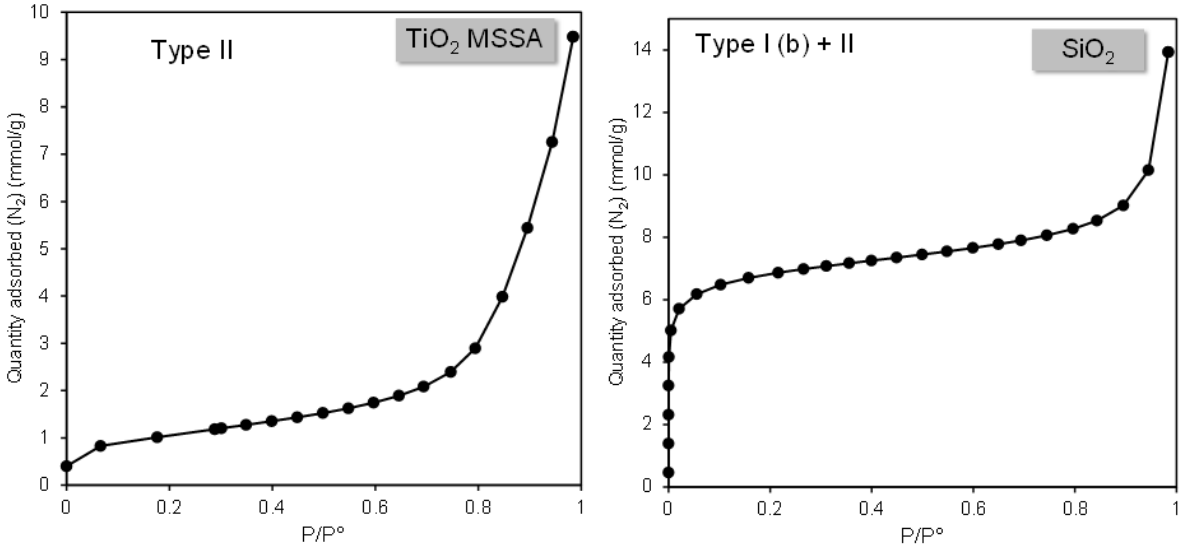


**Fig. 3** Characteristic type II nitrogen adsorption isotherm obtained for $TiO_2$ MSSA and mixed isotherm obtained for $SiO_2$.

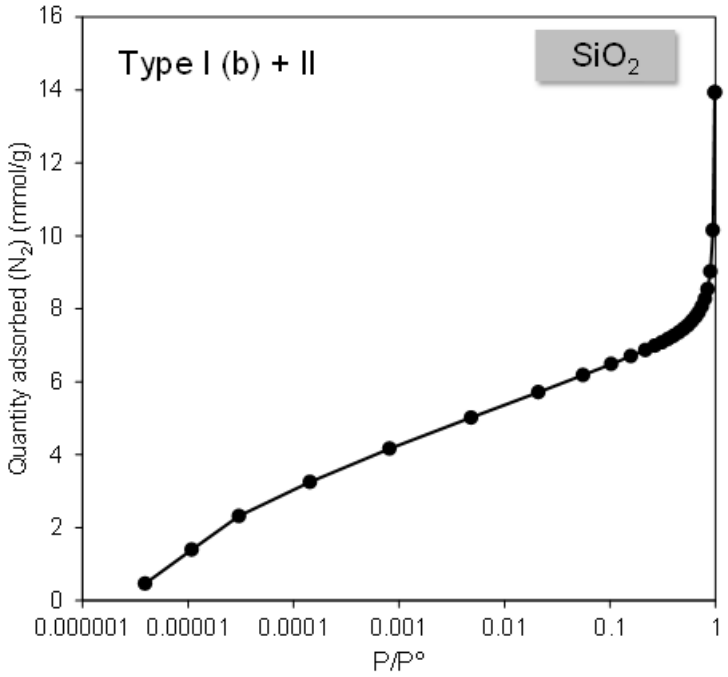


**Fig. 4** $SiO_2$ displaces a mixed nitrogen adsorption isotherm on a semi-log scale.

**Table 3** External specific surface area ($A_{Ex}$), shape factor (D) and VSSA obtained for the eight tested powders.

| Powder | Code | $A_{Ex}$ $m^2/g$ | D | $VSSA_{Cutoff}$ $m^2/cm^3$ | VSSA $m^2/cm^3$ |
|---|---|---|---|---|---|
| $TiO_2$ | LSSA | 9 ± 0.3 | 3 | 60 | 35 |
| | P25 | 55 ± 0.5 | | | 210 |
| | MSSA | 83 ± 0.7 | | | 307 |
| | HSSA | 179 ± 0.4 | | | 701 |
| $SiO_2$ | $SiO_2$ | 87 ± 0.4 | | | 180 |
| $CaCO_3$ | $CaCO_3$ A | 5 ± 0.1 | 1 | 20 | 13 |
| | $CaCO_3$ B | 25 ± 0.3 | 3 | 60 | 64 |
| Activated Carbon Maxsorb® | MSC-30 | 358 ± 41 | 1 | 20 | 788 |

The powders studied had a large diversity of surface areas, with $A_{Ex}$ values between 5 $m^2/g$ and 358 $m^2/g$, spanning almost three orders of magnitude.
The VSSA values obtained were between 13 $m^2/cm^3$ and 923 $m^2/cm^3$. When compared to the $VSSA_{Cutoff}$ values, these values identify the following six powders as nanomaterials: $TiO_2$ MSSA, HSSA and P25, $SiO_2$, $CaCO_3$ B. The remaining two powders ($TiO_2$ LSSA and $CaCO_3$ A) were classed as non-nanomaterials. It should be noted that the VSSA for $CaCO_3$ B (64 $m^2/cm^3$) is very close to the $VSSA_{Cutoff}$ value (60 $m^2/cm^3$).
Interestingly, when we compare all the VSSA values to the $VSSA_{Cutoff}$ of 60 $m^2/cm^3$ (hypothesis D =3), which we would do if the shape of the particles was unknown, the classification remains the same.

### 3.4. Comparison of VSSA, XRD and SEM methods for measurement of constituent particle size

The equivalent mean diameters of the constituent particles determined for the powders, $d_{VSSA}$, from their VSSA were compared to the mean particle diameters $d_{XRD}$ and $d_{SEM}$ determined by XRD and SEM, respectively (figure 5). Amorphous materials were not compared in terms of $d_{XRD}$ as their diffractograms were impossible to exploit. Similarly, the rutile phase of $TiO_2$ P25 was not used in the comparison as the VSSA could not distinguish the crystal phases of the particles and their corresponding sizes and because no rutile was visible (rod-shaped particles) on the SEM images. The sizes determined by the three methods and the bias between the results can be found in Table 4 of the Supplementary Information.
The lowest bias (0%) was obtained for $TiO_2$ MSSA, which had a constituent particle size of 19 nm, and $SiO_2$, with a constituent particle size of 10 nm. The greatest bias was obtained with MSC-30 (-100%). The other biases were between -19% and +31%. The mean bias for all experimental points combined was -12%. Generally, XRD underestimates the particle sizes whereas VSSA biases do not display trend in the discrepancies. The XRD underestimation could be attributed to the Scherrer formula application as the particle shapes are not perfectly spherical. Based on this comparison, MSC-30 is falsely identified as a nanomaterial by VSSA. Indeed, the VSSA classes this activated carbon as a nanomaterial based on its porosity and the shape of the particles (D = 1 for the platelets and a $VSSA_{Cutoff}$ of 20 $m^2/cm^3$). However, the $d_{SEM}$ for carbon is 18 µm with high standard deviation attributed to the difficulty to have repeatable measures of the platelets thickness on the SEM images. This difference can be attributed to the use of the t-plot model which may not be appropriate for this type of material. In contrast, the t-plot model works well for the other microporous powders, $TiO_2$ HSSA and $SiO_2$, for which the bias on particle size was -15% and 6%, respectively. This bias is within the tolerance range ±15 % set. For the other materials in this study, the VSSA ($m^2/cm^3$) correctly classified the powders as nanomaterials or not, as determined by comparison to the reference $d_{SEM}$. Both the VSSA and the SEM methods indicate that $TiO_2$ LSSA and $CaCO_3$ A are not nanomaterials, whereas all the other powders are nanomaterials according to the $d_{SEM}$ or the VSSA. For $CaCO_3$ B, the VSSA (64 $m^2/cm^3$) was close to the $VSSA_{Cutoff}$ (60 $m^2/cm^3$), its classification as a nanomaterial was confirmed by the $d_{SEM}$(94 nm).

These results show that the VSSA could have been used in a reliable way for the studied powders without requiring EM analysis. If only the $VSSA_{Cutoff}$ of 60 $m^2/cm^3$ (hypothesis D =3) is used for comparison with the experimental VSSA data, the classification of the powders as nanomaterials remains correct, except for MSC-30. $TiO_2$ LSSA and $CaCO_3$ A are not nanomaterials and the other powders are nanomaterials according to their $d_{SEM}$.

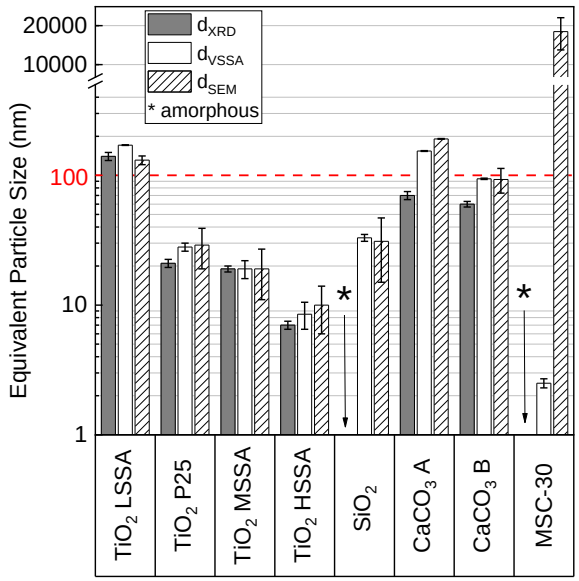


**Fig. 5** : Equivalent particle diameters obtained by VSSA, XRD and SEM methods. The error bars correspond to the standard deviation.

These results corroborate the observations of Wohlleben *et al.* [24] who correctly classified 12 powders as nanomaterials based on their VSSA but could have avoided EM analysis to confirm this classification for the materials they tested. These new data should be considered with caution however because of the broad discrepancies observed. These latter might have been reduced with more replication of experiments or supplementary EM characterization (Transmission Electron Microscopy for instance).

The $d_{XRD}$ values were also compared to the $d_{SEM}$, a mean bias of -25% was found. Once again, the lowest bias (0%) was obtained for $TiO_2$ MSSA, whereas the greatest bias (-63%) was obtained with $CaCO_3$ A. The other biases were between 22% and 57%. These results indicate that XRD can be used in the sole case of spherical and monocrystalline particles to calculate an equivalent particle size. These results agree with the previous study of Weibel *et al* [36]. Therefore, one can consider XRD as a complementary method for particle size determination. Contrary to VSSA, XRD cannot be used without EM analysis for a reliable classification of powders as nanomaterials because of the necessary shape determination (spherical particles) to apply the Sherrer equation.

## 4. Conclusion

In the context of the identification of nanomaterials, this study proposes to compare equivalent particle sizes of eight industrial powders determined by the VSSA, XRD and SEM (reference) methods through a detailed and operational characterisation approach. The results highlight the importance of sample preparation before the gas adsorption and Helium pycnometry measurements, and the careful analysis of the data to determine the VSSA. In particular, the proposed data treatment involves a precise analysis of the gas adsorption isotherms to calculate the external specific surface area for the particles making up the powders, and validation of the Helium pycnometry measurements by comparison with the theoretical density. These two parameters are used to calculate the VSSA for the powder. The comparison of results obtained by the VSSA and SEM methods shows a good correlation in terms of equivalent particle sizes, leading us to conclude the VSSA nanomaterial identification is reliable, although one microporous activated carbon was falsely classified as a nanomaterial based on its VSSA values. In contrast, comparison of the XRD method with the SEM method reveals that the XRD can only reasonably be used to calculate an equivalent particle size when the particles being studied are spherical and monocrystalline. This work provides additional details on the VSSA determination (gas adsorption and Helium Pycnometry) in complement to the recent NanoDefine European project examining the relevance of the VSSA for classification of nanomaterials. The notable results were that no false negatives were obtained with the VSSA method, and that

this parameter appeared to be potentially used for the powder studied without confirmation of the nanomaterial classification with size measurement by EM.
As this work was carried out on a restricted number of materials, this trend should be confirmed testing more substances with the same approach.

## Conflicts of interest

The authors certify there are no conflicts of interest to declare.

## Acknowledgements

We would like to thank E. Jankowska, former member of the Central Institute for Labour Protection (CIOP – Poland) for coordinating with the Nanostruktur laboratory where the scanning electron microscopy images were produced.

## Notes and references

1. M. C. Roco, The long view of nanotechnology development: the National Nanotechnology Initiative at 10 years, *Journal of Nanoparticle Research*, 2011, 13, 427-445.
2. D.T.Leong, Nanosafety Issues of Nanomaterials, in: Reference Module in: Materials Science and Materials Engineering, Elsevier, 2017.
3. S. Foss Hansen, L. R. Heggelund, P. Revilla Besora, A. Mackevica, A. Boldrin and A. Baun, Nanoproducts - what is actually available to European consumers?, *Environmental Science: Nano*, 2016, 3, 169-180.
5. ECHA,https://echa.europa.eu/fr/regulations/nanomaterials.
6. O. Witschger, O. Le Bihan, M. Reynier, C. Durand, A. Marchetto, E. Zimmermann and D. Charpentier, Recommendations for characterizing potential emissions and exposure to aerosols released from nanomaterials in workplace operations, *Hygiène et Sécurité du Travail*, 2012, ND 2355, 41-55.
7. INRS, ED6174, 2014.
8. D. R. Boverhof, C. M. Bramante, J. H. Butala, S. F. Clancy, M. Lafranconi, J. West and S. C. Gordon, Comparative assessment of nanomaterial definitions and safety evaluation considerations, *Regulatory Toxicology and Pharmacology*, 2015, 73, 137-150.
8. EC, Commission recommendation of 18 October 2011 on the definition of nanomaterial, *Official Journal of European Union*, 2011, L275, 38–40.
9. X. Gao and G. V. Lowry, Progress towards standardized and validated characterizations for measuring physicochemical properties of manufactured nanomaterials relevant to nano health and safety risks, *NanoImpact*, 2018, 9, 14-30.
10. Johannes Mielke, Frank Babick, Christian Ullmann and V.-D. Hodoroaba, Evaluation of particle sizing techniques for the implementation of the EC definition of a nanomaterial, presented in the International Congress on Particle Technology, Nuremberg, 2016.
11. F. Babick, J. Mielke, W. Wohlleben, S. Weigel and V.-D. Hodoroaba, How reliably can a material be classified as a nanomaterial? Available particle-sizing techniques at work, *Journal of Nanoparticle Research*, 2016, 18, 158.
12. G. R. Hubert Rauscher, Ana Boix Sanfeliu,, N. G. Hendrik Emons, Robert Koeber,, K. R. Thomas Linsinger, Juan Riego Sintes, and H. S. Birgit Sokull-Klüttgen, Towards a review of the EC Recommendation for a definition of the term “nanomaterial”.Part 3 Scientific-technical evaluation of options to clarify the definition and to facilitate its implementation, European Commission, Joint Research Centre, Institute for Health and Consumer Protection, Italy, 2015.
13. J. Rouquerol and F. Rouquerol, Methodology of Gas adsorption, in: Adsorption by Powders and Porous Solids (Second Edition), Academic Press, Oxford, 2014, pp. 57-104.
14. M. Thommes, K. Kaneko, V. Neimark Alexander, P. Olivier James, F. Rodriguez-Reinoso, J. Rouquerol and S. W. Sing Kenneth, Physisorption of gases, with special reference to the evaluation of surface area and pore size distribution (IUPAC Technical Report), *Pure and Applied Chemistry*, 2015, 87, 1051.
15. V. A. Hackley and A. B. Stefaniak, “Real-world” precision, bias, and between-laboratory variation for surface area measurement of a titanium dioxide nanomaterial in powder form, *Journal of Nanoparticle Research*, 2013, 15, 1742.
16. S.Lowell, Joan E.Shields, M. A.Thomas and a. M. Thommes, Density measurement, in: Characterization of porous solids and powders: surface area, pore size and density, ed. S. S. B. Media, Kluwer Academic Publisher, 2004, ch. 19.
17. Report on the declaration of substances imported, manufactured or distributed in France in 2015, 2016, available to http://www.r-nano.fr.
18. E. Olson, The importance of sample preparation when measuring specific surface area, *Journal of GXP Compliance*, 2012, 16, 52-62.
19. J. Rouquerol, F. Rouquerol, M. Triaca and O. Cerclier, The use of thermal analysis to select the standard outgassing conditions of a set of reference adsorbents, *Thermochimica Acta*, 1985, 85, 311-314.
20. L. Clausen and I. Fabricius, BET Measurements: Outgassing of Minerals, *Journal of Colloid and Interface Science*, 2000, 227, 7-15.

21. ASTM.B923-10, Standard Test Method for Metal Powder Skeletal Density by Helium or Nitrogen Pycnometry, 2010.
22. ISO.12154, Determination of density by volumetric displacement — Skeleton density by gas pycnometry, 2014.
23. A. J. Lecloux, Discussion about the use of the volume-specific surface area (VSSA) as criteria to identify nanomaterials according to the EU definition, *Journal of Nanoparticle Research*, 2015, 17, 447.
24. W. Wohlleben, J. Mielke, A. Bianchin, A. Ghanem, H. Freiberger, H. Rauscher, M. Gemeinert and V.-D. Hodoroaba, Reliable nanomaterial classification of powders using the volume-specific surface area method, *Journal of Nanoparticle Research*, 2017, 19, 61.
25. S. Weigel, P. Müller, K. Löschner, V.D Hodoroaba, M. Stintz, F. von der Kammer, R. Köber and H. Rauscher, NanoDefine - An integrated analytical approach to implement the EC definition of nanomaterial, presented in the International Congress on Particle Technology, Nuremberg, 2016.
26. T. Otowa, R. Tanibata and M. Itoh, Production and adsorption characteristics of MAXSORB: High-surface-area active carbon, *Gas Separation & Purification*, 1993, **7**, 241-245.
27. R. Sharma, D. P. Bisen, U. Shukla and a. B. G. Sharma, X-ray diffraction: a powerful method of characterizing nanomaterials, *Recent Research in Science and Technology*, 2012, 4, 77-79.
28. S. Bau, O. Witschger, F. Gensdarmes, O. Rastoix and D. Thomas, A TEM-based method as an alternative to the BET method for measuring off-line the specific surface area of nanoaerosols, *Powder Technol*, 2010, 200.
29. P.-J. De Temmerman, J. Lammertyn, B. De Ketelaere, V. Kestens, G. Roebben, E. Verleysen and J. Mast, Measurement uncertainties of size, shape, and surface measurements using transmission electron microscopy of near-monodisperse, near-spherical nanoparticles, *Journal of Nanoparticle Research*, 2013, 16, 2177.
30. P.-J. De Temmerman, E. Van Doren, E. Verleysen, Y. Van der Stede, M. A. D. Francisco and J. Mast, Quantitative characterization of agglomerates and aggregates of pyrogenic and precipitated amorphous silica nanomaterials by transmission electron microscopy, *Journal of Nanobiotechnology*, 2012, 10, 24.
31. K. S. W. Sing, F. Rouquerol and J. Rouquerol, Classical Interpretation of Physisorption Isotherms at the Gas–Solid Interface, in: Adsorption by Powders and Porous Solids (Second Edition), Academic Press, Oxford, 2014, pp. 159-189.
32. J. Rouquerol, P. Llewellyn and F. Rouquerol, Is the bet equation applicable to microporous adsorbents?, in: Studies in Surface Science and Catalysis, eds. P. L. Llewellyn, F. Rodriquez-Reinoso, J. Rouqerol and N. Seaton, Elsevier, 2007, vol. 160, pp. 49-56.
33. F. Rouquerol, L. Luciani, P. Llewellyn, R. Denoyel and J. Rouquerol, *Techniques de l'ingénieur Surfaces et structures fonctionnelles*, 2003, TIB534DUO.
34. K. S. W. Sing, F. Rouquerol, P. Llewellyn and J. Rouquerol, Assessment of Microporosity, in: Adsorption by Powders and Porous Solids (Second Edition), Academic Press, Oxford, 2014, pp. 303-320.
35. A. Weibel, R. Bouchet, F. Boulc and P. Knauth, The Big Problem of Small Particles: A Comparison of Methods for Determination of Particle Size in Nanocrystalline Anatase Powders, *Chemistry of Materials*, 2005, 17, 2378-2385.